

Primljen / Received: 2.9.2019.

Ispravljen / Corrected: 19.12.2019.

Prihvaćen / Accepted: 5.1.2020.

Dostupno online / Available online: 10.8.2020.

# Indirect green façade as an overheating prevention measure

## Authors:



**Valentina Lesjak**, MSc. CE  
University of Ljubljana, Slovenia  
Faculty of Civil and Geodetic Engineering  
Department of Buildings and Construction Complexes  
[valentina.lesjak94@gmail.com](mailto:valentina.lesjak94@gmail.com)



**Luka Pajek**, MSc. CE  
University of Ljubljana, Slovenia  
Faculty of Civil and Geodetic Engineering  
Department of Buildings and Construction Complexes  
[luka.pajek@fgg.uni-lj.si](mailto:luka.pajek@fgg.uni-lj.si)

Corresponding author



Assist.Prof. **Mitja Košir**, PhD. Arch.  
University of Ljubljana, Slovenia  
Faculty of Civil and Geodetic Engineering  
Department of Buildings and Construction Complexes  
[mitja.kosir@fgg.uni-lj.si](mailto:mitja.kosir@fgg.uni-lj.si)

Research paper

**Valentina Lesjak, Luka Pajek, Mitja Košir**

## Indirect green façade as an overheating prevention measure

Simulation and experimental investigation of the indirect green façade (IGF) impact on thermal behaviour of buildings is presented in the paper. The study was conducted in Punat, Krk, Croatia, in the summer of 2018. The IGF reduced the incident solar radiation by up to 505 W/m<sup>2</sup> and façade temperatures by up to 13.5 K. Experimental results were used to simulate the indoor thermal comfort of a simple building model. When IGF was positioned across the entire sun-exposed wall, an average decrease of operative temperature was up to 6 K for a new house and up to 5 K for a traditional stone house.

### Key words:

vertical greenery systems, indirect green façade, solar radiation, façade surface temperature, operative temperature

Prethodno priopćenje

**Valentina Lesjak, Luka Pajek, Mitja Košir**

## Indirektna zelena fasada kao mjera za sprečavanje pregrijavanja

U radu je prikazana simulacija i eksperimentalno istraživanje utjecaja indirektno zelene fasade (IZF) na toplinsko ponašanje zgrade. Istraživanje je provedeno na lokaciji Punat na otoku Krku u Hrvatskoj tijekom ljeta 2018. godine. Primjenom IZF-a utjecaj sunčevog zračenja smanjen je do 505 W/m<sup>2</sup>, a temperatura na vanjskoj površini fasade smanjene su do 13,5 K. Eksperimentalni su rezultati korišteni za simuliranje toplinske ugodnosti u unutrašnjosti zgrade primjenom jednostavnog modela. Kada je IZF postavljen preko čitavog zida izloženog suncu, prosječno smanjenje operative temperature iznosilo je do 6 K za novu zgradu, tj. do 5 K za tradicionalnu kamenu kuću.

### Ključne riječi:

vertikalni vrtni sustavi, indirektna zelena fasada, Sunčevo zračenje, površinska temperatura fasade, operativna temperatura

Vorherige Mitteilung

**Valentina Lesjak, Luka Pajek, Mitja Košir**

## Fassadenbegrünung als Maßnahme gegen Überhitzung

In der Abhandlung werden eine Simulation und eine experimentelle Untersuchung des Einflusses einer Fassadenbegrünung auf das Wärmeverhalten des Gebäudes dargestellt. Die Untersuchung wurde in Kroatien am Standort Punat auf der Insel Krk während des Sommers 2018 durchgeführt. Durch Anwendung einer Fassadenbegrünung wurde der Einfluss der Sonneneinstrahlung um bis zu 505 W/m<sup>2</sup> gesenkt, und die Temperatur an der Außenfläche der Fassade wurde um bis zu 13.5 K gesenkt. Die experimentellen Ergebnisse wurden verwendet, um den thermischen Komfort im Inneren des Gebäudes durch Anwendung eines einfachen Modells zu simulieren. Als die Fassadenbegrünung über die gesamte Wand angebracht wurde, die der Sonne ausgesetzt ist, betrug die Senkung der Betriebstemperatur bis zu 6 K für das neue Gebäude, d. h. bis 5 K für ein traditionelles Steinhaus.

### Schlüsselwörter:

vertikale Gartensysteme, Fassadenbegrünung, Sonneneinstrahlung, Oberflächentemperatur der Fassade, Betriebstemperatur

### 1. Introduction

In our increasingly globalised and united world more than a half of the world population (55 %) lives in urbanised areas [1]. In Europe, the share of population living in cities is even higher and currently amounts to 74 %. In conjunction with technological development and economic growth, a high level of urbanisation is one of the main reasons for radical increase of global energy use in the last four decades [1]. The International Energy Agency [2] states that, on an average, the total global final energy use increased until 2017 by more than two times compared to the year 1971. A substantial share of total global energy is used by buildings in order to maintain indoor thermal and visual comfort [3] making building energy efficiency and low environmental impact two of the greatest challenges of the construction industry. For this reason, new building technologies and materials have been constantly developed, with a focus on indoor environmental quality affecting the choice of building envelope [4]. Constant longing to develop more energy efficient, environmentally friendly, and comfortable buildings has encouraged architects and designers to incorporate green surfaces into building envelopes [5], which have positive impact on building performance especially during cooling season.

Horizontal greenery systems have been studied ever since the 1960s when new materials and technology started to revamp green roof design with increased efficiency [6], and are presently developed almost to perfection. Therefore, the attention of designers shifted to the integration of vertical greenery in buildings. Although plants have been spontaneously climbing vertical surfaces since the time of very first construction activities, deliberate cultivation of plants on these surfaces has only begun in recent decades. Vertical greenery systems (VGS) can bring numerous effects that are beneficial to the building envelope, such as shading, cooling

due to evaporation, additional insulation, and reducing wind speeds [7]. Among these, thermal benefits of VGS have been the most broadly empirically investigated [8]. In addition to the stated benefits, VGS also shield the façade surface from ultraviolet radiation, rain, extreme temperature fluctuations and moisture, and can improve acoustic comfort while also increasing the real-estate value [5, 9]. At the urban level, the use of VGS may reduce air pollution and accumulation of dust and heavy metals, improve health and well-being of city dwellers [10], and increase urban biodiversity [11]. VGS can be divided into four basic groups according to the wall assembly design and position of vegetation, as shown in Figure 1.

Although there are many different types of VGS, the indirect green façade (IGF) ranks among the simplest solutions, because it is easily constructed (in many cases as a separate construction) and does not require much maintenance. Several studies have been made about the effect of VGS on buildings. Wong et al. [12] investigated eight different VGS and discovered that the interaction between the leaf surface area, geometry and colour, on the one hand, and microclimatic conditions, such as solar radiation on the other, is complex and can result in different cooling capabilities during the day and at night. For example, in their study the capability of IGF to reduce the façade surface temperature compared to the case without IGF was 4.4 K. Similar conclusions were drawn by Pérez et al. [13] who investigated the impact of IGF using the *Wisteria sinensis* plant (a deciduous vine) where, on an average, surface temperatures were reduced by 5.5 K and up to 15.2 K in August and September when IGF was used. Comparable results were presented in many other studies using different plants in various climates (see references [14–25]). Overall, the surface temperature reduction due to application of VGS was predominantly related to the plant type (i.e. leaf surface area) and climatic conditions (i.e. humidity, air temperature, and intensity of solar radiation).

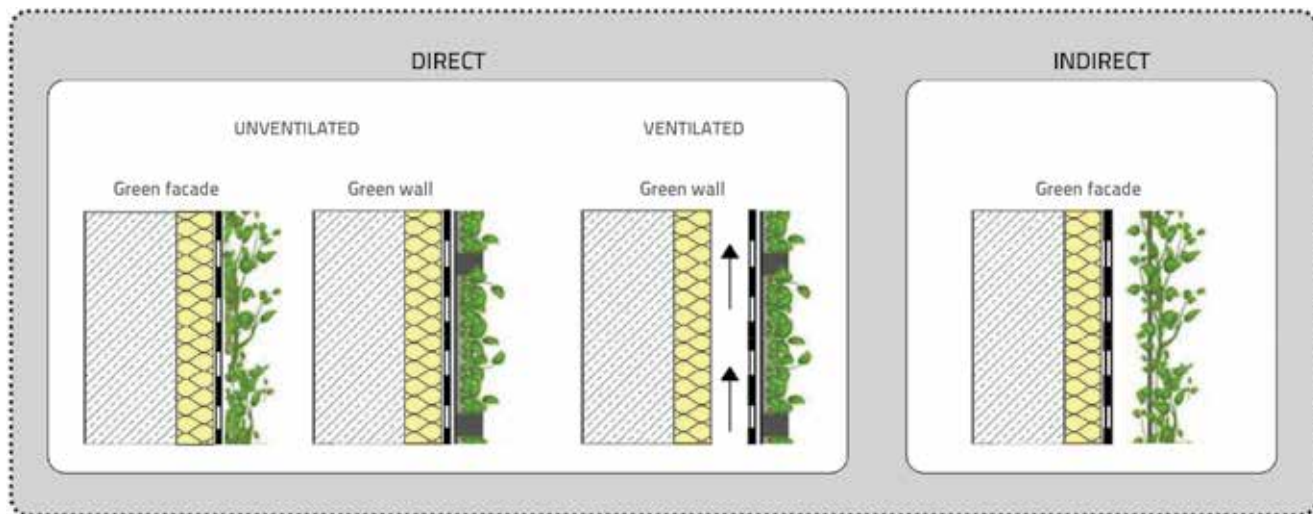


Figure 1. Classification of vertical greenery systems

Several studies additionally investigated the effect of IGF on indoor conditions and energy use of buildings. In their study conducted in a dry Mediterranean Continental climate, Pérez et al. [13] showed that the indoor air temperature was reduced by 1.5 K when the plant was fully developed during summer. In the experimental cubicle studied by Coma et al. [16] in the Mediterranean climate, the indoor air temperature in September was reduced by 1 K when the IGF was used. However, the daily cooling energy use was reduced only by 1 % in July (50 % covered wall, cooling set-point 24 °C). The opposite was shown in a hot arid climate by Pérez et al. [21] where a 34 % reduction of electrical energy was measured during cooling season for a leaf area index (LAI) of 3.5–4.0. All the above-mentioned studies investigated the impact of IGF on building envelope and indoor thermal conditions. However, little is known about the behaviour of such green systems in the transitional areas between temperate and Mediterranean climates, such as the Kvarner Gulf. This area has in particular been shown to be of high interest for investigation of potential bioclimatic building design strategies, especially during cooling season [26]. Therefore, the research presented in this paper took place on the island of Krk in Croatia, where an experimental IGF was constructed. The focus of the presented

research was to construct a simple, easy-to-assemble, low-cost IGF in order to experimentally analyse its impact on the incidence of solar irradiance and external surface temperatures in case of a building with a conventional External Thermal Insulating Contact System (ETICS) façade. In addition, the thermal comfort of a hypothetical living environment (i.e. living room) was evaluated by EnergyPlus simulations for three different configurations of IGF and two building envelope types. The purpose of the research is to contribute to better understanding of the behaviour and influence of IGF on the façade surface and indoor thermal environment of buildings in the investigated area.

## 2. Experimental part

### 2.1. Methodology

The experimental part of the study was conducted in the city of Punat (N 45°01'; E 14°63'; 15 m a.s.l.) on the island of Krk in Croatia from 16 June to 30 October 2018. The experiment was conducted on a part of a recently built residential building. The external wall of the building is composed of the 30 cm thick brick load bearing structure, and 8 cm of the polystyrene

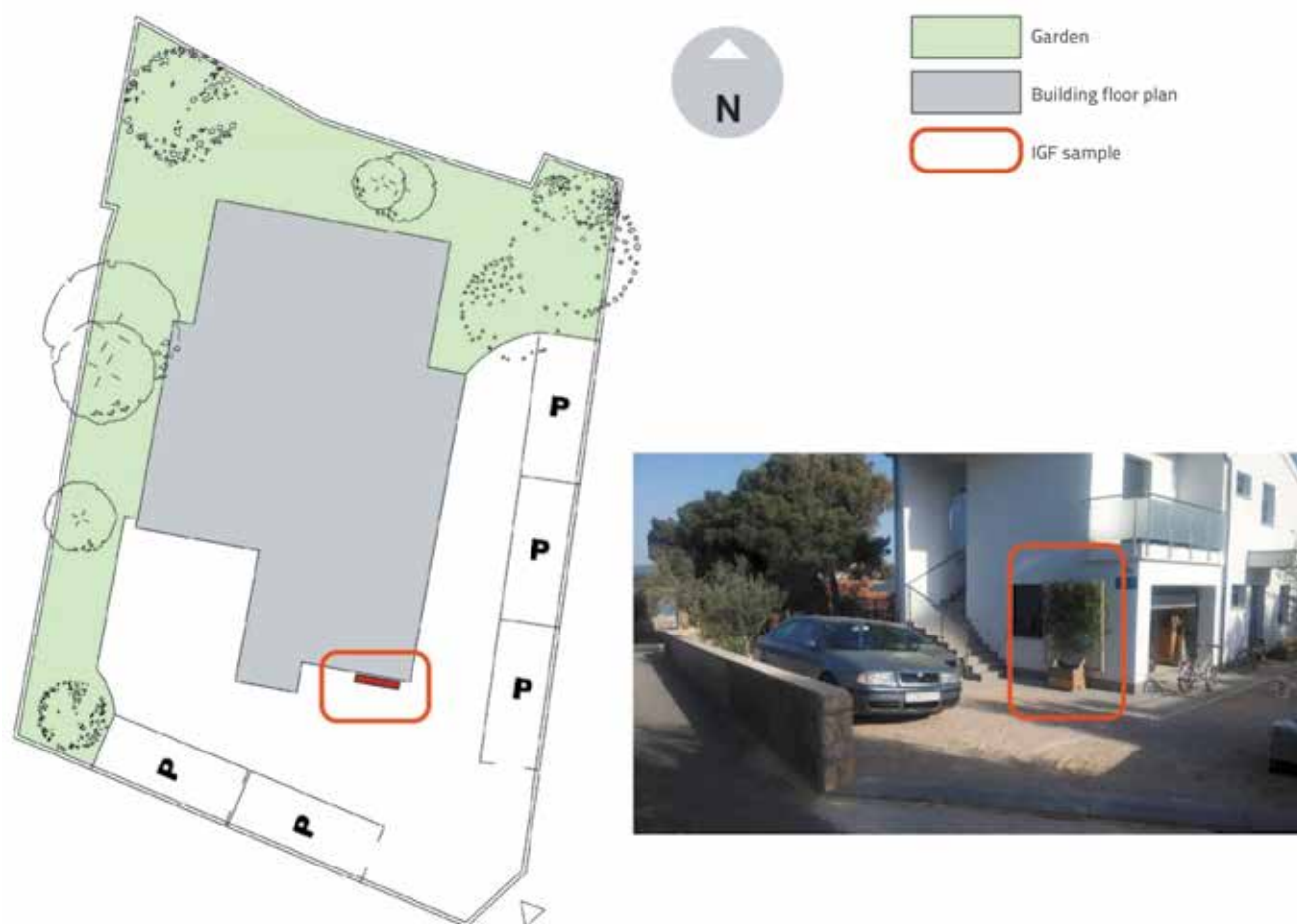
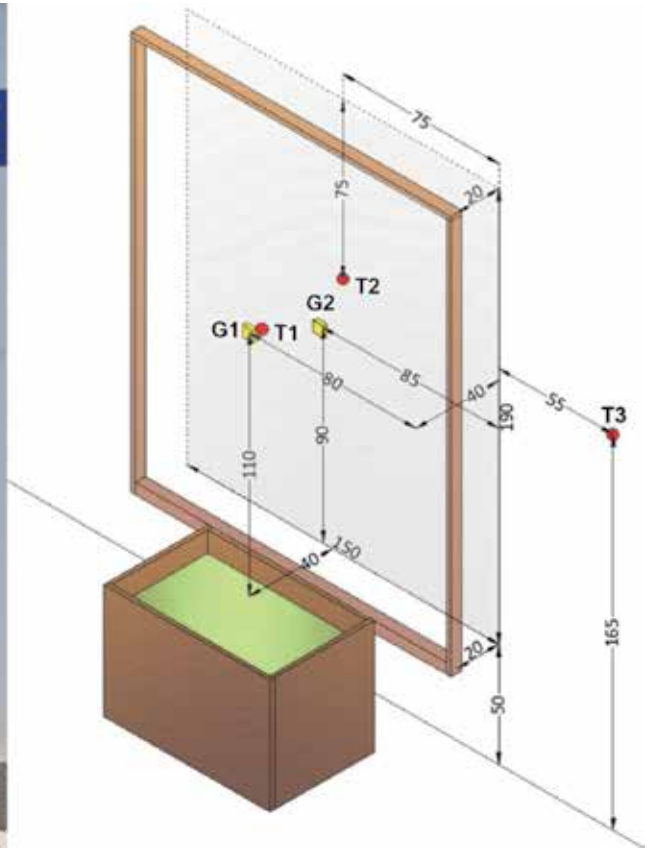


Figure 2. Experimental IGF location (left) and the position of IGF sample relative to the southern façade of the building (right)



T1	°C	air temperature in the IGF plant layer
T2	°C	air temperature at facade surface behind the IGF
T3	°C	air temperature at facade surface
G1	W/m <sup>2</sup>	solar radiation in front of the IGF
G2	W/m <sup>2</sup>	solar radiation behind the IGF

Figure 3. Setup of IGF experiment and positions of measuring points

(EPS) thermal insulation with a white-coloured ETICS. For the purpose of the experiment, an IGF sample was constructed. In order to minimize the effect of the surroundings (i.e. shading) on the measurements, the experimental IGF was positioned next to the southern façade, as shown in Figure 2. The IGF sample (Figure 3) consisted of a plant container, supporting structure, and a plant. The supporting structure was constructed as a modular wooden trellis system with additional rope supports, while the plant container was made of wooden bars insulated with plastic membrane on the inside. Because the aim was to maximise the effect of IGF during the summer and to minimise it during the winter, a deciduous Chinese wisteria (i.e. *Wisteria sinensis*) plant was used.

The IGF sample was positioned so that there was a continuous 15 cm gap between the ETICS façade surface and the plant, which allowed for air circulation (Figure 3). The branches, which grew towards the façade, were constantly “helped” so that they can wrap around the supporting trellis to maintain an unobstructed airflow. The sides were closed using perforated fabric in order to imitate a continuous IGF, namely the fabric










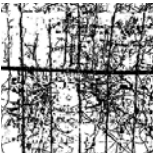
acted as a side obstacle for the sun, while the airflow was not prevented.

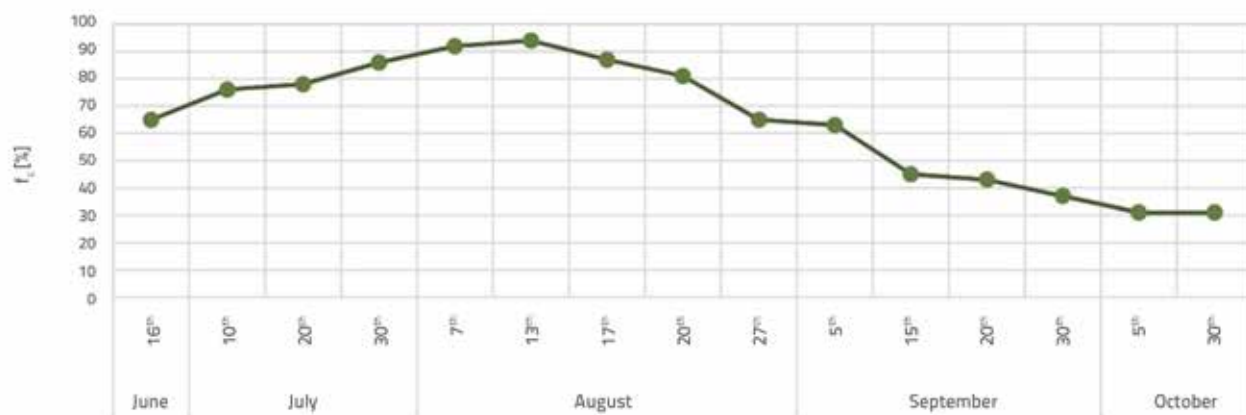
Thermocouples and solar cells were used to evaluate the effect of IGF on air temperature at façade surface (°C) and the intensity of solar radiation (W/m<sup>2</sup>). All the measurements were recorded using Almemo-2690-8a data logger. Additionally, a simple video camera was used to monitor sky conditions. All ambient data, such as air temperature (°C), relative air humidity (%), wind speed (m/s), and precipitation (mm), were acquired from the local weather station located 2 km away. Global horizontal solar radiation (G3) was measured in an unobstructed horizontal plane nearby. Measuring points on and behind the IGF are shown in Figure 3. The plant development was constantly observed and recorded using a camera. The photos were subsequently processed to calculate the percentage of façade coverage –  $f_c$ .

## 2.2. General experimental results

As mentioned in Section 2.1, the  $f_c$  was constantly monitored during the period of the experiment because, as the plant

Table 1. Plant overgrowth and leaf coverage ratio over time

	16 <sup>th</sup> June	20 <sup>th</sup> July	13 <sup>th</sup> August	5 <sup>th</sup> September	30 <sup>th</sup> October
Photo of plant overgrowth					
Photo negative of plant overgrowth					
Calculated $f_c$	65 %	78 %	94 %	63 %	31 %

Figure 4. Variation of percentage of façade coverage ( $f_c$ ) during experimentTable 2. Average monthly solar radiation in G1, G2 and G3, average monthly air temperature at façade surface behind IGF – T2 and on the unshaded façade surface – a T3. Characteristic differences of  $\Delta T$  and  $\Delta G$  between 12 pm and 3 pm are also presented

		June	July	August	September	October
$G_{avg}$ [ $W/m^2$ ]	G1	/*	/*	477.7	585.7	483.7
	G2	/*	/*	107.8	260.7	331.4
	G3	/*	653.6	581.9	544.6	315.0
	$\Delta G_{avg}$	/*	/*	370.0	325.0	152.2
T2 [ $^{\circ}C$ ]	Min.	17.8	25.1	15.7	18.0	16.1
	Max.	35.0	39.2	40.5	37.4	38.1
	Avg.	29.4	31.7	33.5	30.5	28.5
T3 [ $^{\circ}C$ ]	Min.	18.4	26.4	15.4	20.3	16.1
	Max.	42.9	48.8	49.1	44.4	40.3
	Avg.	32.9	39.8	42.0	38.2	30.0
$\Delta T$ [K]	Min.	-0.8	1.3	-0.4	0.5	-0.2
	Max.	10.7	10.5	12.3	12.1	3.1
	Avg.	3.5	8.1	8.5	7.7	1.6

\* In June and July 2018, G measuring points were moved to optimum positions and so the results are not shown for this period as they would not be representative.

grows, the plant overgrowth and leaf density greatly influence the shading capability of the IGF. The results are presented in Table 1 and Figure 4.

The maximum façade coverage was 94 % when the plant was fully-grown, while the minimum  $f_c$  was 31 %, which was the result of shading induced by the plant branches and trellis (Table 1).

For the purposes of this study, the temperature and solar radiation were monitored at several different points. Subsequently, the differences in temperature ( $\Delta T = T3 - T2$ ) and solar radiation ( $\Delta G = G1 - G2$ ) were calculated. The representative results are shown in Table 2. These values are given for the period between 12 pm and 3 pm since it is characterized by a fairly uniform maximum radiation and a uniform difference ( $\Delta T$ ) between the temperature of façade behind the IGF (T2) and the temperature of the reference point on the façade (T3).

The measured solar radiation behind the plant (G2) depends on the plant overgrowth and its ability to intercept solar radiation. In August, when the plant is fully-grown ( $f_c > 80 \%$ ), G2 value is at its lowest. The situation is quite the opposite in October when the plant loses the leaves ( $f_c < 40 \%$ ) and the G2 value is at its highest. Therefore, the decrease of  $\Delta G$  follows the percentage of façade coverage as a consequence of leaf loss of the plant. Beside the effect on the received solar radiation,

the IGF greatly mitigates the fluctuation of the façade surface temperature over time. The sun-exposed façade is 12 K warmer during August than in October, while the IGF shaded façade is only 5 K warmer.

### 2.3. Specific results for hot summer period

Based on analysis of the average monthly outdoor air temperature ( $\theta_{avg}$ ), the outdoor relative humidity ( $RH_{avg}$ ), G1,  $\Delta G$ , T3 and  $\Delta T$ , the period between 5 and 15 August 2018 was selected to represent the IGF influence. The highest outdoor air temperature ( $\theta_{max}$ ) was achieved during the mentioned period, although it was characterized by a variety of weather events, namely there were very hot days with clear sky, but also days with rain. During this period, the  $\theta_{max}$  did not exceed 35 °C, while  $\theta_{min}$  did not drop below 20 °C. RH values varied according to the outdoor air temperature ( $\theta$ ) and weather conditions. Measurement results for the representative period are shown in Figure 5. On days with clear sky, the recorded average  $\Delta G$  value between 12 pm and 3 pm ranged between 410 and 465 W/m<sup>2</sup>. This points to the ability of the plant to prevent a considerable share of solar radiation from penetrating through the IGF layer of leaves and branches. However,  $\Delta G$  was significantly smaller on overcast days because the intensity of solar radiation is greatly affected by cloudiness. In particular, an average  $\Delta G$

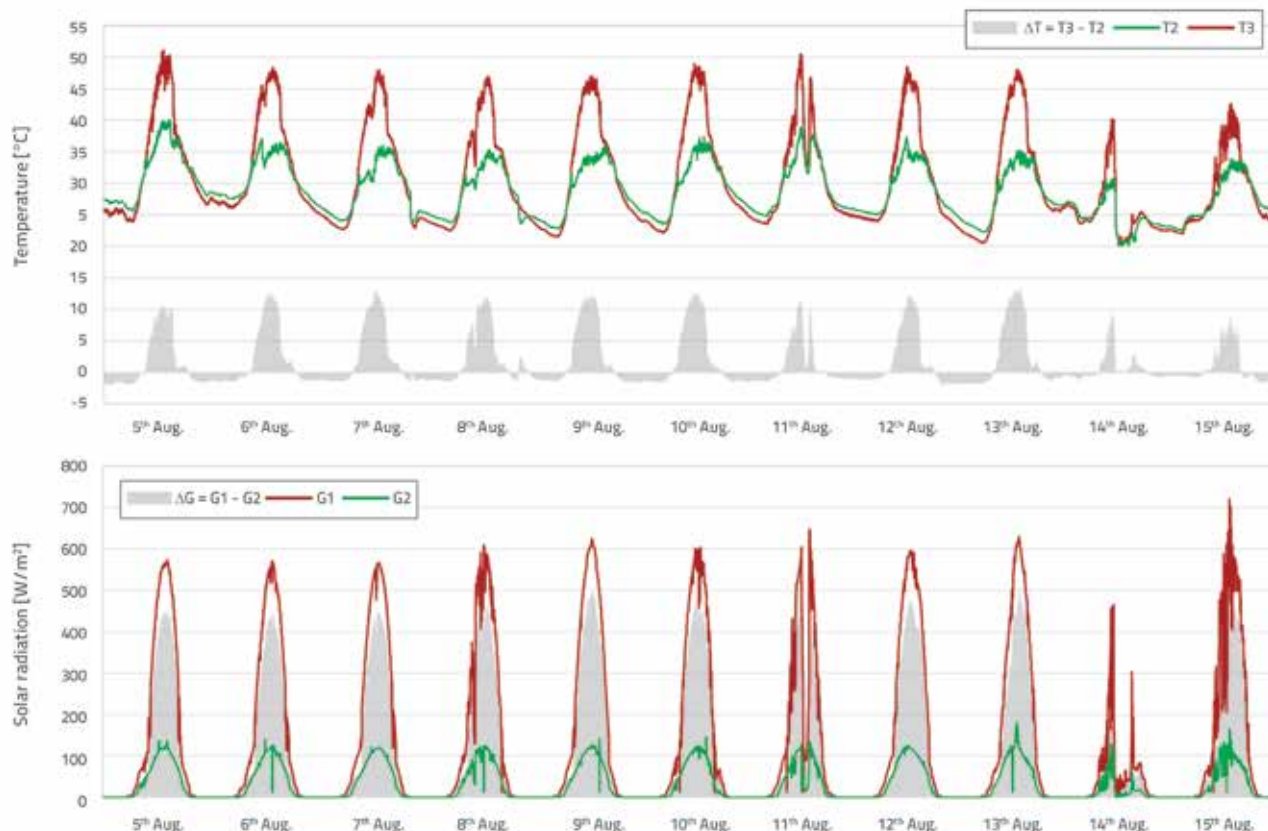


Figure 5. Recorded temperature and solar radiation values and corresponding differences in front of and behind IGF during reference period (5-15 August 2018)

measured on 14 August was only  $28 \text{ W/m}^2$ , while it was  $425.3 \text{ W/m}^2$  on 8 August (Figure 5).

On clear days, the maximum  $\Delta T_{\text{avg}}$  values (Figure 5) are relatively high and range from  $9.5 \text{ K}$  to  $12.3 \text{ K}$ . On overcast days, the  $\Delta T$  values vary to a higher extent, as cloud density and time of cloudiness are strongly reflected in the values. Thus, between 12 pm and 3 pm, maximum average  $\Delta T$ s range from  $0.2 \text{ K}$  to  $11.0 \text{ K}$ . During the nighttime ( $\Delta T_{\text{avg}}$  (20:00–6:59)), when  $T_2$  is higher than  $T_3$ , inversion occurs and  $\Delta T$  averages between  $-0.6$  and  $-1.7 \text{ K}$  (Figure 5). It should be highlighted that a greater difference between the maximum daytime  $\theta$  and minimum nighttime  $\theta$  results in a higher  $\Delta T$  at night. It is assumed that  $T_3$  responds quicker than  $T_2$  to the change in  $\theta$ , since the plant acts as a thermal barrier and slows down the change of temperature at  $T_2$ . The relationship between  $\Delta T$  and  $\Delta G$  is shown in Figure 6.  $\Delta G$  is almost constant for  $\Delta G$  values of approximately  $50 \text{ W/m}^2$  (i.e. when the measuring device is still in shade). However,  $\Delta T$  increases rapidly as the outside air temperature increases. The reason for this behaviour is that the thermocouple is positioned in the immediate vicinity of the corner adjacent to the eastern façade. This side of the façade is directly sunlit even when the thermocouple is still in shadow, causing  $T_3$  to rise while simultaneously  $\Delta G$  stagnates. For the values of  $\Delta G$  above  $50 \text{ W/m}^2$ , the sun begins to irradiate the plant directly so that, in addition to  $\Delta T$ ,  $\Delta G$  begins to increase. When  $\Delta G$  is high, the  $\Delta T$  is also high, showing the additional effect of solar radiation on the resulting temperature at  $T_3$ , while  $T_2$  is not affected by solar radiation because the IGF intercepts most incidence radiation. The described behaviour demonstrates that the impact of the IGF on the resulting surface façade temperature is mostly due to the shading effect of the plant, rather than to the cooling effect due to evaporation.

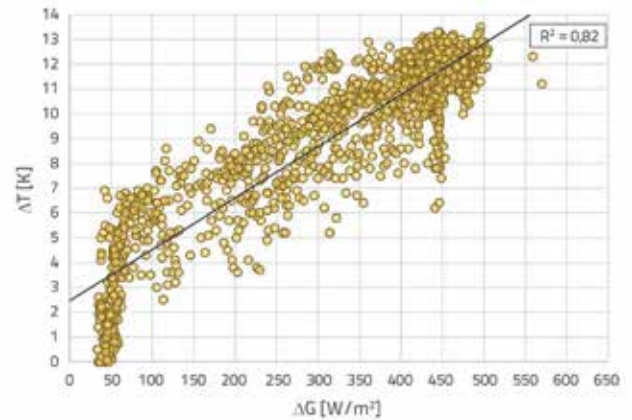


Figure 6. Relation between  $\Delta T$  and  $\Delta G$  on clear days during reference period

### 2.3.1. Typical hot sunny day – 9 August

Figure 7 shows distribution of solar radiation over a typical hot sunny day. The maximum measured global horizontal solar radiation ( $G_3$ ) of  $766 \text{ W/m}^2$  was recorded at 1:18 pm, which corresponds to the solar noon on the particular day. Compared to  $G_3$ , the  $G_1$  was about 20 % lower ( $G_{1\text{max}} = 625 \text{ W/m}^2$ ) owing to the apparent position of the sun in the hemisphere. However, the effect of the IGF is reflected in the achieved value of  $G_2$  ( $G_{2\text{max}} = 122 \text{ W/m}^2$ ), which was further reduced compared to  $G_3$  and  $G_1$ . The IGF sample is shaded by the building itself until 10 am due to its orientation. Until then, the measurements at points  $G_1$  and  $G_2$  are mainly a result of the diffuse solar radiation component. After 10 am the sun is directly irradiating the plant, and so  $G_1$  values start to rise rapidly. In contrast,  $G_2$  values rise steadily even when the sun begins to irradiate the plant. The reason for

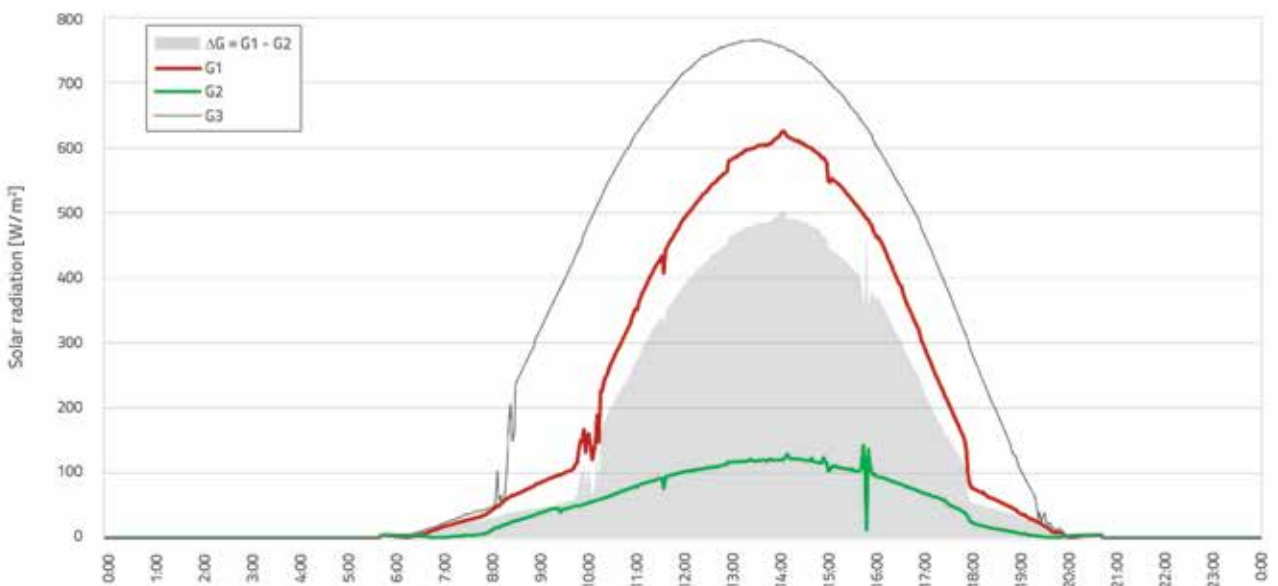


Figure 7. Solar radiation on 9 August 2018 – typical hot sunny day

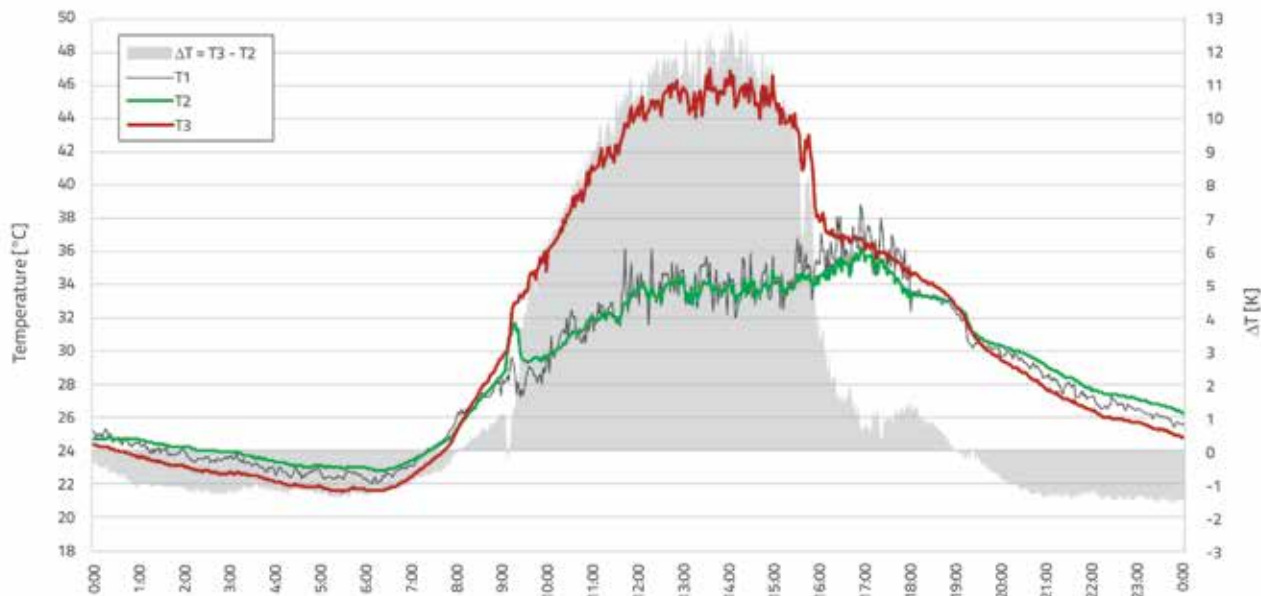


Figure 8. Temperatures on 9<sup>th</sup> of August 2018 – a typical hot sunny day

such behaviour is that the solar radiation, measured at the G2 measuring point, mainly consists of the diffuse component of solar radiation. The value of G2 was always less than G1, which shows that the IGF intercepts a considerable amount of solar radiation. At the time of the maximum achieved value of G1, the G2 amounts to only 18 % of G1, while in the morning and evening, when the plant is not directly sunlit, this fraction is up to 55 %. The reason for the various effectiveness of the IGF on the reduction of received solar radiation lies in the greater impact of the plant on the reduction of the direct component of solar radiation compared to the diffuse component.

Temperature fluctuations measured on a particular day are shown in Figure 8. At night, all measured temperatures were

close to the  $\theta$ . During the daytime, however, they increased due to the impact of solar radiation. The highest temperatures were expectedly recorded at T3 with values above 45 °C, which is by 14.0 K higher than  $\theta$ .

It can be seen in Figure 8 that temperatures of the façade behind the IGF are much lower. Nevertheless, they continuously rise during the daytime when solar radiation is strong. The maximum temperature registered at T2 did not exceed 36 °C, which is still 5.0 K above the  $\theta$ . The maximum  $\Delta T$  during the considered day was 12.9 K, recorded at 2 pm, which corresponds to maximum values of T3 (45.9 °C) and G1 (620 W/m<sup>2</sup>). In the morning and in the evening,  $\Delta T$  values were substantially lower, while they were negative during the nighttime. The reason for the latter is

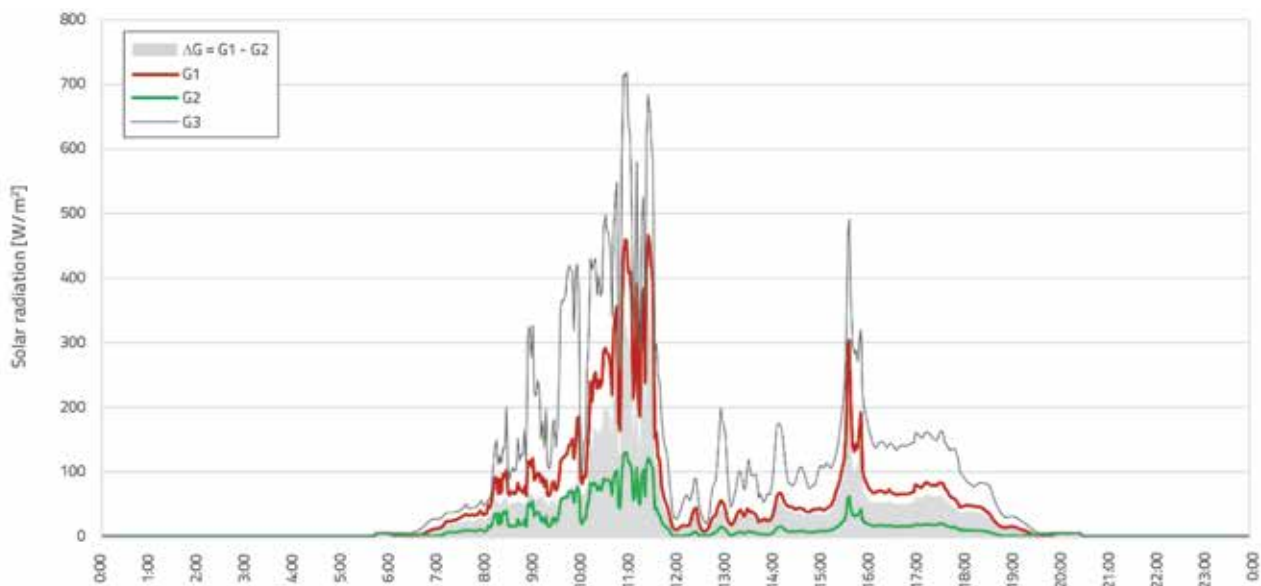


Figure 9. Solar radiation on 14 August 2018 – typical hot overcast day with a rain event





Figure 10. Temperatures on 14 August 2018 – typical hot overcast day with a rain event

that the plant acts as a tampon layer, which slows down heat transfer and reduces radiation losses from the façade surface, thus maintaining T2 slightly above T3.

### 2.3.2. Typical hot overcast day with rain event – 14 August

Figure 9 shows distribution of solar radiation over a typical hot overcast day with an intermittent rain event (i.e. thunderstorm). In the forenoon, the clouds blocked substantial part of the incoming solar radiation resulting in low G1, G2 and G3 values. Later when the rain started (around noon), all values dropped further due to extreme cloudiness, namely the G3 value to 19.5 W/m<sup>2</sup>, G1 to 9.5 W/m<sup>2</sup> and G2 to less than 1.0 W/m<sup>2</sup>. The values of G1 and G3 fluctuated depending on the ratio of sunlight transmitted through the clouds, while G2 represented only 10 to 30 % of G1 value as a consequence of the influence of the IGF. Therefore, ΔG was still non-zero and ranged between 6 and 35 W/m<sup>2</sup>.

Figure 10 shows temperature fluctuations on the observed day. The rain caused the drop of T1, T2 and T3 below the  $\theta$ . Because the precipitation was intercepted by the plant, the rain did not directly wet the façade behind it. As a result, the façade behind the plant cooled down slower and T2 was higher than T3, which means that ΔT was negative during that time. However, during the dry part of the day, ΔT remained positive, but with almost negligible difference with regard to T3.

## 3. Thermal performance simulation

### 3.1. Methodology

The purpose of this paper was to verify the effect of an IGF on the internal thermal conditions of a residential building in the

climatic context of the analysed location (i.e. Punat, Croatia). Therefore, the effect of IGF was simulated using a simple model of a living room as a part of a residential building. The model was constructed using Design Builder software [27] and simulated with EnergyPlus. Because of the location of the experiment, the model size was determined on the basis of *Croatian Rules on minimum technical conditions for the design and construction of apartments included in the Social Housing Construction Programme* [28], from where minimum living room and window space dimensions were sourced (see Figure 14a). The window was assumed to be a single panoramic opening measuring 1.3 by 2.0 m, resulting in the window to wall ratio (WWR) of 16.7 %. The model has only one external façade that is exposed to sun. All other surfaces of the model were defined as adiabatic in order to exclude heat exchange between internal surfaces of the building. The simulation of thermal response was made for three different orientations of the sun-exposed façade, namely south, southwest, and west. The occupancy was defined as 2 people with a default Design Builder occupancy schedule for the living room (150 W total internal heat gain power) and the electric lighting power was set to 5 W/m<sup>2</sup>.

The simulation of thermal response was performed for two different configurations of external wall. The first one represented a traditional stone construction [29] typical for older buildings constructed in the considered location, while the second one had a new thermally insulated external wall with ETICS (see Table 3) corresponding to Croatian national legislation requirements ( $U < 0.45 \text{ W/m}^2\text{K}$ ) [30]. The absorptivity ( $\alpha$ ) of the external façade rendering was in both instances presumed to be 0.4 (Table 3), corresponding to a light-coloured surface like beige, cream, sand, etc. [31]. The energy plus weather (EPW) climate data for Punat was prepared using a web weather

Table 3. Characteristics of two considered external wall configurations

Building type	External wall	U [W/m²K]	α [-]	Glazing	U [W/m²K]	g [-]
Traditional stone house	Natural stone wall	2.53	0.4	Double glazed window without low-e coating and with air filling	3.16	0.69
New thermally insulated house	Brick wall with 6 cm of EPS (λ = 0.035 W/m²K) external thermal insulation	0.42	0.4	Triple glazed window with low-e coating and argon filling	0.79	0.47

file generator developed by the Joint Research Centre of the European Commission [32]. The file was generated according to the measured hourly data for the period between 2005-2014. Table 3 presents the thermal (U value) and optical (g factor) properties for glazing considered in the simulation.

The ventilation of the simulation model was presumed to be natural and was set to 0.8 h<sup>-1</sup>, which is a sum of minimal air flow for residential buildings (0.5 h<sup>-1</sup> [33]) and uncontrolled infiltration of 0.3 h<sup>-1</sup>. For the purpose of this paper, the conditioning of the building, namely heating and cooling, was disabled, and so the building was in the so-called “free-run”. The operative temperature (T<sub>o</sub>) was observed as an indoor thermal environment parameter. The operative temperature provides a better insight into the quality of indoor thermal comfort than just the air temperature, since it also contains the impact of the mean radiant temperature of the indoor environment. The latter component can significantly affect a person’s perception of thermal comfort indoors [34].

The impact of IGF on the thermal response of the model was defined as a shading component with a time-dependent shading factor (f<sub>sh</sub>). Based on the experimental measurement results the solar transmittance of the shading component was set to be equal to the IGF defined as f<sub>p</sub> as shown in Eq. (1).

$$f_p = \frac{G_2}{G_1} \tag{1}$$

The value of f<sub>p</sub> = 1.0 means that the plant transmits all of the G<sub>1</sub> to the façade and the value of f<sub>p</sub> = 0.0 means that the plant intercepts all of the G<sub>1</sub> and that the façade is 100 % shaded. Figure 11 shows the determined f<sub>p</sub> factor as a function of the experimentally measured G<sub>1</sub> value.

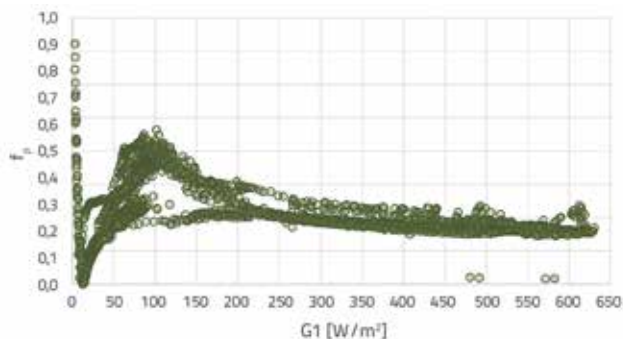


Figure 11. f<sub>p</sub> factor as a function of G1 on sunny days in reference period

However, as the solar radiation (i.e. G<sub>1</sub> and G<sub>2</sub>) was not monitored throughout the whole year, the necessary annual f<sub>p</sub> values were determined using the percentage of façade coverage (f<sub>c</sub>) determined according to the plant overgrowth. Therefore, available experimentally determined transmittance factors (f<sub>p</sub>) were correlated with the percentage of façade coverage (f<sub>c</sub>), as can be seen in Figure 12. G<sub>1</sub> and G<sub>2</sub> values registered between 12 pm and 3 pm were considered for the calculation of f<sub>p</sub>. The correlation can be described by the exponential trend curve with a R<sup>2</sup> = 0.90. The exponential trend curve can be described by Eq. (2).

$$f_p = 0,1681 \cdot f_c^{-1,269} \tag{2}$$

The Eq. (2) only applies to f<sub>c</sub> values higher than 30 %, since lower values of f<sub>c</sub> do not occur due to the presence of bare branches of the plant and the supporting trellis construction.

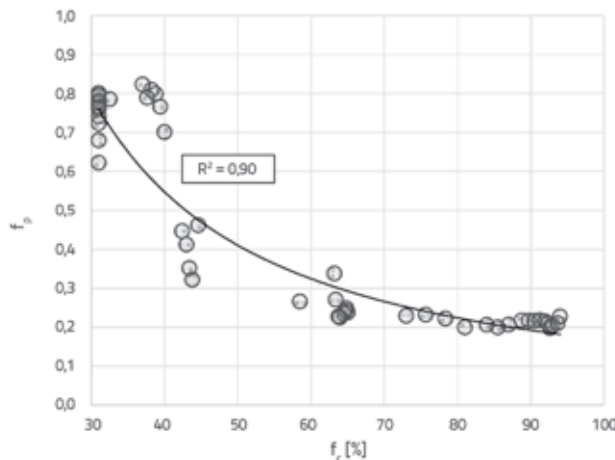


Figure 12. Correlation between f<sub>p</sub> and f<sub>c</sub>

The shading factor f<sub>sh</sub> was then calculated using Eq. (3) for every day of the month throughout the entire year. The values of f<sub>sh</sub> between October and April are constant at 0.28, because the plant is deciduous and there are no leaves.

$$f_{sh} = 1 - f_p \tag{3}$$

Accordingly, the influence of the IGF on the shading of façade was described with a fractional schedule of f<sub>sh</sub> depending on the day of the month, as shown in Figure 13.

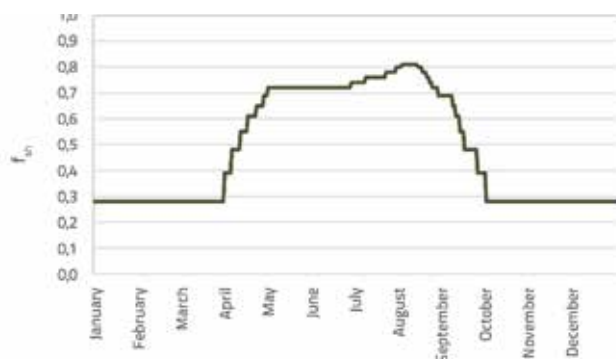


Figure 13. Monthly development of  $f_{sh}$  used in thermal simulations

One of the objectives was also to analyse the impact of different IGF configurations, and so three different configurations of IGF were defined. The first configuration included an IGF mounted exclusively in front of the glazing (Figure 14b). In the second configuration, the IGF was set only in front of the opaque wall, excluding the glazing (Figure 14c), while in the case of the third one the IGF covered the entire surface of the external façade (Figure 14d). In all the cases, IGF was positioned in such a way to form a 20 cm gap between itself and the surface of the building façade. All of the configurations were compared with the baseline model without the IGF (Figure 14a).

### 3.2. Simulation results

The simulation results are presented in Table 4 and Figures 15 and 16, where fluctuations of operative temperature ( $T_o$ ) in the living room in free-run operation throughout the year is shown. A plant that intercepts solar radiation decreases the external surface temperature and heat influx through the wall. Therefore, it can be clearly seen (Figures 15 and 16) how the installation of the IGF in front of the building

external surface affects  $T_o$  in the summer as well as in the winter. Accordingly, a decrease in resulting  $T_o$  can be observed. However, the efficiency of IGF highly depend on the degree of plant overgrowth, represented in the simulations as  $f_{sh}$ . For instance, during summer, when the plant is fully grown, the decrease in  $T_o$  as an effect of the IGF is the largest. In contrast, during winter when the plant discards the leaves, the impact of the IGF on the  $T_o$  is minimal. A typical impact of the IGF on the  $T_o$  is determined as the difference between the average  $T_o$  in the case of the baseline model (i.e. without the IGF), average  $T_o$ , and the  $T_o$  of various IGF configurations and orientations (Table 4). In the case of a traditional stone house (Figure 15), the impact of IGF on indoor operative temperature is significant during summer, when  $T_o$  typically decreases by 3–6 K if IGF is applied. The results show that the efficiency (i.e. the decrease in  $T_o$ ) of IGF was the highest for the southwest orientation. This is due to the concurrence of high solar radiation intensity and lower incidence angles at this orientation, while the external air temperature is still high. This effect was previously demonstrated by Košir et al. [35] for overheating analysis of a building shaded using conventional mechanical shading devices in a temperate location of Ljubljana.

It can be seen in Figure 15 that during summer the effect of IGF is the lowest for south orientation, whereas during the winter, the south orientation is affected the most. As expected,  $T_o$  decreases the most when IGF covers the entire surface of the façade (i.e. IGF wall, see Figure 14d) for all orientations. On the other hand, when IGF is applied either only over the glazing (i.e. IGF,glazing) or solely over the opaque part of the wall (i.e. IGF,opaque), the  $T_o$  decreases, surprisingly, almost to the same extent (Figure 15). However, because older stone houses typically have a lower glazing ratio than specified in the model, it could be concluded that installing an IGF in front of the opaque part of the wall (i.e.

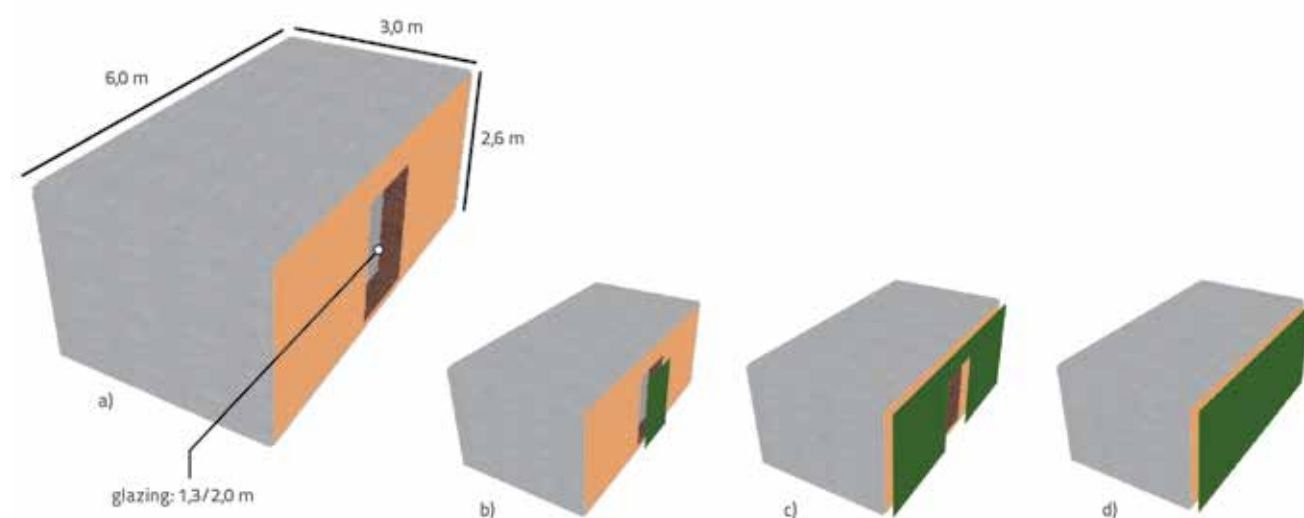


Figure 14. a) baseline model; b) IGF only in front of the glazing (IGF,glazing); c) IGF only in front of the opaque wall (IGF,opaque); d) IGF covers the entire external surface (IGF, wall)

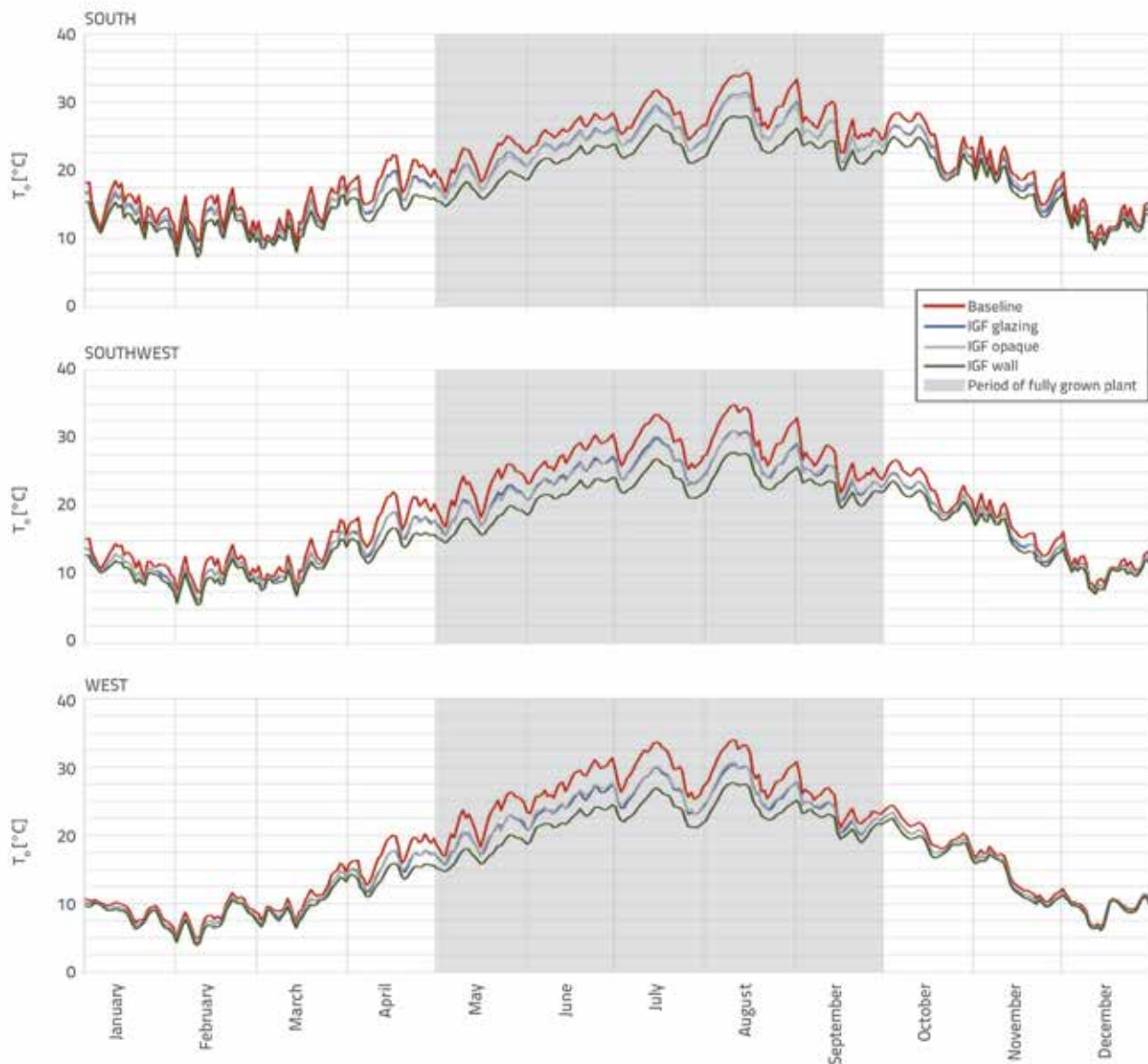


Figure 15. Operative temperature ( $T_o$ ) fluctuations throughout the year for different IGF configurations for a traditional stone house in Punat at south, southwest, and west orientations

IGF, opaque in Figure 15) may have greater potential for reducing the operative temperature in the case of traditional buildings with high façade U values. In the case of the new thermally insulated house (Figure 16) the results follow a similar trend. However, they differ in the achieved impact exerted by the IGF. Because in this instance the opaque part of the wall is more thermally insulated, the installation of IGF in front of the glazing (i.e. IGF, glazing) has greater effect on the  $T_o$  in comparison to the IGF, opaque. If the IGF is installed in front of the entire wall (i.e. IGF, wall), the average  $\Delta T_o$  for the most promising southwest orientation is up to 5.0 K for a new house and up to 6.3 K for a traditional one (Table 4). Although such installation might be problematic as we cover the glazing and consequentially

affect the daylighting and views, the results demonstrate that operative temperature can be significantly reduced during the summer by applying the IGF. In particular, in the case of the IGF,wall,  $T_o$  is in most cases within the limits of thermal comfort (i.e. below 26 °C [33]) without any mechanical cooling applied. It can also be deduced from Figures 15 and 16 that thermal behaviour and the impact of the IGF of the two studied houses depends on thermal transmittance of the external wall. The indoor environment in a traditional stone house with no thermal insulation is strongly influenced by external conditions, resulting in prominent fluctuations of  $T_o$  (Figure 15). In contrast, in a new house with proper thermal insulation the interaction with outdoor environment is reduced, which results in a more stable  $T_o$  (Figure 16).

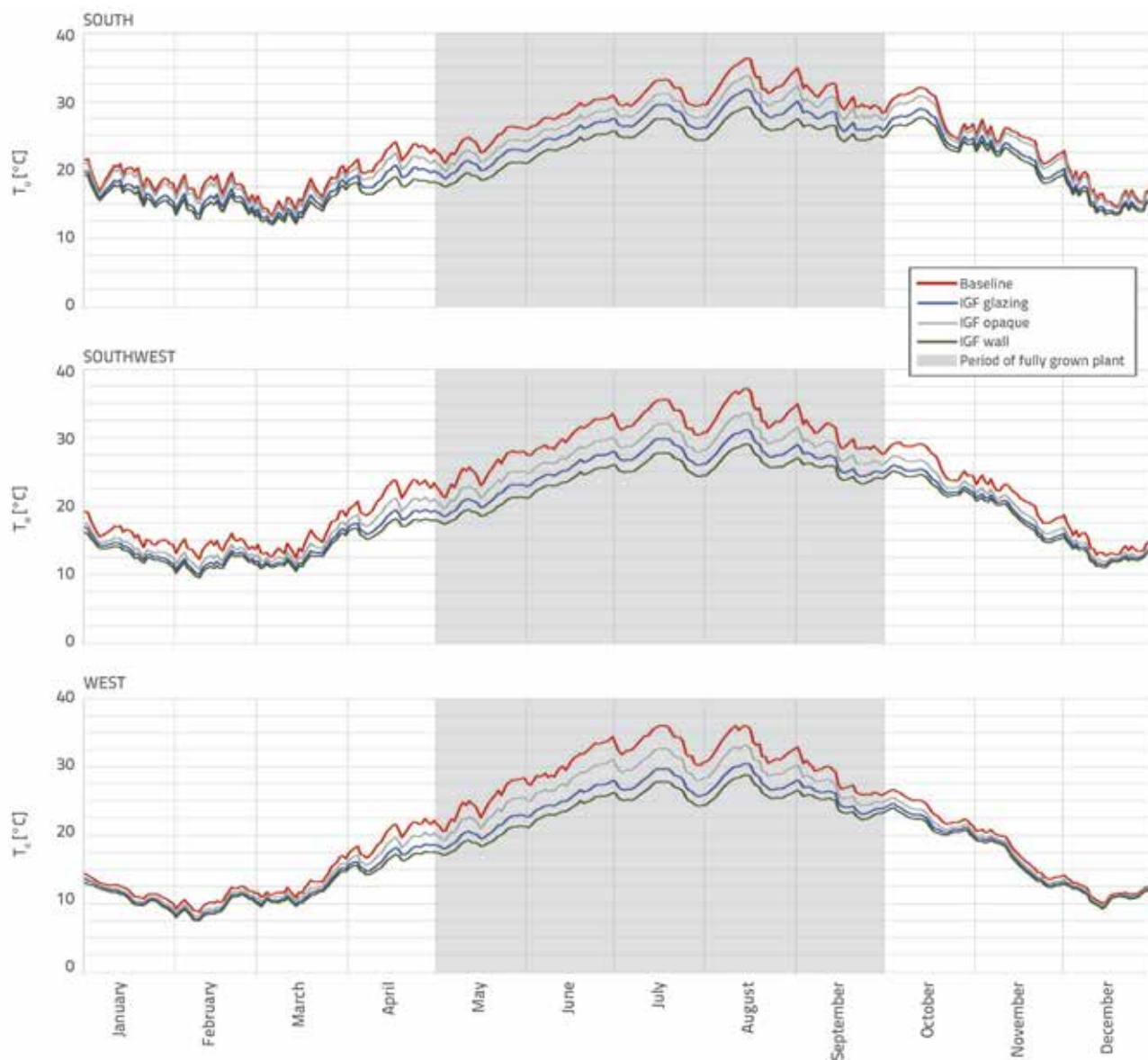


Figure 16. Operative temperature ( $T_o$ ) fluctuations throughout the year for different IGF configurations for a new thermally insulated house in Punat at south, southwest and west orientations

Table 4. Average impact of IGF on the decrease of indoor operative temperature ( $T_o$ ) from 1 May to 30 September (i.e. the time of a fully-grown plant during a hot part of the year)

Façade orientation	Building type	$\Delta T_o$ . "IGF, glazing" [K]		$\Delta T_o$ . "IGF, opaque" [K]		$\Delta T_o$ . "IGF, wall" [K]	
		Avg.	Max.	Avg.	Max.	Avg.	Max.
South	Traditional stone house	2.1	4.1	2.3	3.9	4.4	8.1
	New thermally insulated house	3.5	5.5	1.8	2.7	5.3	8.2
Southwest	Traditional stone house	2.7	4.8	2.7	4.3	5.0	8.1
	New thermally insulated house	4.7	6.9	2.7	4.0	6.3	9.0
West	Traditional stone house	2.6	4.9	2.4	4.2	4.7	8.1
	New thermally insulated house	4.6	7.0	2.4	3.7	5.9	8.9

## 4. Discussion

The aim of the research was to determine the effect of the indirect green façade (IGF) on the building envelope and indoor thermal environment using experimental measurements and thermal simulations. As a deciduous plant, Chinese wisteria showed the ability to intercept solar radiation on both sunny and overcast days. Nevertheless, the calculated transmittance factor ( $f_p$ ) indicated that the selected plant had a greater shading ability under higher solar radiation values. In the case of clear sky conditions, the value of the solar radiation behind the plant represented only 20 % to 30 % of the received solar radiation in front of the plant, namely the incident solar radiation was reduced by up to 500 W/m<sup>2</sup>. Even on overcast days, the IGF intercepted 70–90 % of received solar radiation. However, the absolute values were lower in these cases and therefore the impact of IGF was almost irrelevant. Temperature measurements showed that the surface temperature of the sun-exposed façade attained values as high as 52.1 °C. In contrast, the surface temperature of the façade behind the IGF was never above 40.3 °C. Moreover, the average effect of IGF, expressed as  $\Delta T$ , was 9.5–12.3 K on sunny days during the selected analysed period, while the maximum measured  $\Delta T$  was 13.5 K. Similar impacts were reported by other studies (see refs. [13, 16, 19, 21, 23]). The experimental results demonstrated that IGF also acted as a heat screen at night as temperatures behind the plant were on average 1.5 K higher than in front of it. The recorded night-time inversion is a phenomenon that has also been reported in other studies [23, 36]. Reducing solar radiation and surface temperature is crucial in the hot part of the year. At that time, the sun-exposed façade can be under a strong effect of solar radiation. The high façade surface temperatures pose a risk of material degradation and higher indoor temperatures, effectively increasing the building's energy consumption due to use of mechanical cooling [37].

Simulation results revealed that IGF has a great potential for passive increase of the summer-time thermal comfort in buildings by reducing the indoor operative temperature ( $T_o$ ). When IGF was used,  $T_o$  decreased on an average by 1.8–6.3 K, which generally means that thermal comfort of the occupants is satisfactory (i.e. operative temperature below 26 °C). This effect is particularly desirable in the summer when it is crucial to prevent overheating in homes. Overall, the best results were achieved when the IGF was installed in front of the entire external wall. However, the effect of IGF was highly dependant on the IGF configuration with respect to the building envelope,

and on its thermal properties and façade orientation. In the case of the traditional stone house, it was shown that positioning the IGF in front of the glazing or in front of the opaque part of the wall resulted in almost the same reduction of  $T_o$ . In case of the new thermally insulated house, the effect was greater if IGF was positioned in front of the glazing for all façade orientations. In general, the IGF was most effective for the southwest orientation in all configurations. However, the IGF was more efficient when it was used for shading the new thermally insulated house. Therefore, based on simulation results, it can be confirmed that IGF can be used to improve thermal comfort and potentially reduce the need for cooling indoor environment during the summer.

## 5. Conclusion

To summarize, the results of the study show that indirect green façade (IGF) can be used as an effective overheating prevention measure in buildings exposed to weather conditions, such as those prevailing in the Kvarner Gulf in Croatia. However, the findings of the study are only valid in general terms. Each building should therefore be considered separately. Punat is a coastal village, where outdoor temperatures during summer are high throughout the day and night, while there are also many sunny days. In locations where the influence of solar radiation on overheating is greater than the influence of outdoor air temperatures, the IGF may have even greater effect, since it was experimentally determined that the IGF affects the resulting surface temperatures predominantly through shading. The simplified thermal simulations were not used to calculate the absolute value of the effect, but rather to study the behaviour of the IGF-influenced building in free-run operation, so as to clearly present passive influence of the IGF on thermal response of buildings. It should finally be highlighted that the effect of various ventilation strategies, such as draft, stack or night ventilation, were not considered in the simulations, which would affect the overall impact of IGF.

## Acknowledgements

The authors acknowledge financial support provided by the Slovenian Research Agency (research core funding No. P2-0158). We would also like to extend our thanks to Marko Jankovec, Boštjan Glažar and Jože Stepan from the Faculty of Electrical Engineering, University of Ljubljana, for their advice and provision of measuring equipment.

## REFERENCES

- [1] Department of Economic and Social Affairs, World Urbanization Prospects: The 2018 Revision, 2018.
- [2] IEA. World energy balances 2017, <https://www.iea.org/statistics/balances/>, 23.08.2019.
- [3] Besir, A.B., Cuce, E.: Green roofs and facades: A comprehensive review, *Renew Sustain Energy Rev*, 82 (2018), pp. 915–939, <https://doi.org/10.1016/j.rser.2017.09.106>.
- [4] Farid, F.H.M., Ahmad, S.S., Raub, A.B.A., Shaari, M.F.: Green "Breathing Facades" for Occupants' Improved Quality of Life, *Procedia - Soc Behav Sci*, 234 (2016), pp. 173–184, <https://doi.org/10.1016/j.sbspro.2016.10.232>.

- [5] Vox, G., Blanco, I., Schettini, E.: Green façades to control wall surface temperature in buildings, *Build Environ*, 129 (2018), pp. 154–166, <https://doi.org/10.1016/j.buildenv.2017.12.002>.
- [6] Jim, C.Y.: Green roof evolution through exemplars: Germinal prototypes to modern variants, *Sustain Cities Soc*, 35 (2017), pp. 69–82, <https://doi.org/10.1016/j.scs.2017.08.001>.
- [7] Pérez, G., Rincón, L., Vila, A., González, J.M., Cabeza, L.F.: Green vertical systems for buildings as passive systems for energy savings, *Appl Energy*, 88 (2011), pp. 4854–4859, <https://doi.org/10.1016/j.apenergy.2011.06.032>.
- [8] Radić, M., Brković Dodig, M., Auer, T.: Green Facades and Living Walls—A Review Establishing the Classification of Construction Types and Mapping the Benefits, *Sustainability*, 11 (2019) 17, pp. 4579–4602, <https://doi.org/10.3390/su11174579>.
- [9] Pérez, G., Coma, J., Martorell, I., Cabeza, L.F.: Vertical Greenery Systems (VGS) for energy saving in buildings: A review, *Renew Sustain Energy Rev*, 39 (2014), pp. 139–165, <https://doi.org/10.1016/j.rser.2014.07.055>.
- [10] Ottelé, M., van Bohemen, H.D., Fraaij, A.L.A.: Quantifying the deposition of particulate matter on climber vegetation on living walls, *Ecol Eng*, 36 (2010), pp. 154–162, <https://doi.org/10.1016/j.ecoleng.2009.02.007>.
- [11] Mayrand, F., Clergeau, P.: Green Roofs and Green Walls for Biodiversity Conservation: A Contribution to Urban Connectivity?, *Sustainability*, 10 (2018) 4, pp. 985–998, <https://doi.org/10.3390/su10040985>.
- [12] Wong, N.H., Kwang Tan, A.Y., Chen, Y., Sekar, K., Tan, P.Y., Chan, D., i suradnici: Thermal evaluation of vertical greenery systems for building walls, *Build Environ*, 45 (2010), pp. 663–672, <https://doi.org/10.1016/j.buildenv.2009.08.005>.
- [13] Pérez, G., Rincón, L., Vila, A., González, J.M., Cabeza, L.F.: Behaviour of green facades in Mediterranean Continental climate, *Energy Convers Manag*, 52 (2011), pp. 1861–1867, <https://doi.org/10.1016/j.enconman.2010.11.008>.
- [14] Perini, K., Ottelé, M., Fraaij, A.L.A., Haas, E.M., Raiteri, R.: Vertical greening systems and the effect on air flow and temperature on the building envelope, *Build Environ*, 46 (2011), pp. 2287–2294, <https://doi.org/10.1016/j.buildenv.2011.05.009>.
- [15] Koyama, T., Yoshinaga, M., Hayashi, H., Maeda, K., Yamauchi, A.: Identification of key plant traits contributing to the cooling effects of green façades using freestanding walls, *Build Environ*, 66 (2013), pp. 96–103, <https://doi.org/10.1016/j.buildenv.2013.04.020>.
- [16] Coma, J., Pérez, G., Solé, C., Castell, A., Cabeza, L.F.: New Green Facades as Passive Systems for Energy Savings on Buildings, *Energy Procedia*, 57 (2014), pp. 1851–1859, <https://doi.org/10.1016/j.egypro.2014.10.049>.
- [17] Cameron, R.W.F., Taylor, J.E., Emmett, M.R.: What's 'cool' in the world of green façades? How plant choice influences the cooling properties of green walls, *Build Environ*, 57 (2014) 57, pp. 198–207, <https://doi.org/10.1016/j.buildenv.2013.12.005>.
- [18] Jim, C.Y.: Thermal performance of climber greenwalls: Effects of solar irradiance and orientation, *Appl Energy*, 57 (2015) 57, pp. 631–643, <https://doi.org/10.1016/j.apenergy.2015.05.077>.
- [19] Hoelscher, M.-T., Nehls, T., Jänicke, B., Wessolek, G.: Quantifying cooling effects of facade greening: Shading, transpiration and insulation, *Energy Build*, (2016) 114, pp. 283–90, <https://doi.org/10.1016/j.enbuild.2015.06.047>.
- [20] Ottelé, M., Perini, K.: Comparative experimental approach to investigate the thermal behaviour of vertical greened façades of buildings, *Ecol Eng*, 108 (2017), pp. 152–161, <https://doi.org/10.1016/j.ecoleng.2017.08.016>.
- [21] Pérez, G., Coma, J., Sol, S., Cabeza, L.F.: Green facade for energy savings in buildings: The influence of leaf area index and facade orientation on the shadow effect, *Appl Energy*, 187 (2017), pp. 424–437, <https://doi.org/10.1016/j.apenergy.2016.11.055>.
- [22] Grabowiecki, K., Jaworski, A., Niewczas, T., Belleri, A.: Green Solutions - Climbing Vegetation Impact on Building - Energy Balance Element, *Energy Procedia*, 111 (2017), pp. 377–386, <https://doi.org/10.1016/j.egypro.2017.03.199>.
- [23] Vox, G., Blanco, I., Schettini, E.: Green façades to control wall surface temperature in buildings. *Build Environ*, 129 (2018), pp. 154–166, <https://doi.org/10.1016/j.buildenv.2017.12.002>.
- [24] Yang, F., Yuan, F., Qian, F., Zhuang, Z., Yao, J.: Summertime thermal and energy performance of a double-skin green facade: A case study in Shanghai, *Sustain Cities Soc*, 39 (2018), pp. 43–51, <https://doi.org/10.1016/j.scs.2018.01.049>.
- [25] Cameron, R.W.F., Taylor, J., Emmett, M.: A Hedera green façade - Energy performance and saving under different maritime-temperate, winter weather conditions, *Build Environ*, 92 (2015), pp. 111–121, <https://doi.org/10.1016/j.buildenv.2015.04.011>.
- [26] Pajek, L., Košir, M.: Can building energy performance be predicted by a bioclimatic potential analysis? Case study of the Alpine-Adriatic region, *Energy Build*, 139 (2017), pp. 160–173, <https://doi.org/10.1016/j.enbuild.2017.01.035>.
- [27] DesignBuilder Software Ltd - Home 2019, <https://designbuilder.co.uk/>. 26.07.2019.
- [28] Pravilnik minimalnih tehničkih uvjeta za projektiranje i gradnju stanova iz Programa društveno poticane stanogradnje - NN 106/04, NN 25/06, NN 121/11 2011.
- [29] Živković, Z.: Tradicijska kamena kuća dalmatinskog zaleđa: priručnik za obnovu i turističku valorizaciju, Ministarstvo turizma Republike Hrvatske, Ministarstvo vanjskih i europskih poslova, Zagreb, 2015.
- [30] Tehnički propis o racionalnoj uporabi energije i toplinskoj zaštiti u zgradama - NN 128/15, NN 70/18 2018.
- [31] Hudobivnik, B., Pajek, L., Kunič, R., Košir, M.: FEM thermal performance analysis of multi-layer external walls during typical summer conditions considering high intensity passive cooling, *Appl Energy*, 178 (2016), pp. 363–375, <https://doi.org/10.1016/j.apenergy.2016.06.036>.
- [32] European Commission. TMY Generator 2019, <https://re.jrc.ec.europa.eu/pvgis5/tmy.html>, 21.07.2019.
- [33] EN 15251:2010. Indoor environmental input parameters for design and assessment of energy performance of buildings addressing indoor air quality, thermal environment, lighting and acoustics, 2010.
- [34] Dovjak, M., Shukuya, M., Krainer, A.: Connective thinking on building envelope - Human body exergy analysis, *Int J Heat Mass Transf*, 90 (2015), pp. 1015–1025, <https://doi.org/10.1016/j.ijheatmasstransfer.2015.07.021>.
- [35] Košir, M., Gostiša, T., Kristl, Ž.: Influence of architectural building envelope characteristics on energy performance in Central European climatic conditions, *J Build Eng*, 15 (2018), pp. 278–288, <https://doi.org/10.1016/j.job.2017.11.023>.
- [36] Yang, F., Yuan, F., Qian, F., Zhuang, Z., Yao, J.: Summertime thermal and energy performance of a double-skin green facade: A case study in Shanghai, *Sustain Cities Soc*, 39 (2018), pp. 43–51, <https://doi.org/10.1016/j.scs.2018.01.049>.
- [37] Košir, M., Pajek, L., Igljić, N., Kunič, R.: A theoretical study on a coupled effect of building envelope solar properties and thermal transmittance on the thermal response of an office cell, *Sol Energy*, 174 (2018), pp. 669–682, <https://doi.org/10.1016/j.solener.2018.09.042>.